

## Article

# Options for Methane Fuel Processing in PEMFC System with Potential Maritime Applications

Eun-Shin Bang <sup>1</sup>, Myoung-Hwan Kim <sup>2</sup> and Sang-Kyun Park <sup>3,\*</sup><sup>1</sup> Department of Marine Engineering, Korea Maritime and Ocean University, Busan 49112, Republic of Korea<sup>2</sup> Division of Marine System Engineering, Korea Maritime and Ocean University, Busan 49112, Republic of Korea<sup>3</sup> Division of Maritime AI & Cyber Security, Korea Maritime and Ocean University, Busan 49112, Republic of Korea

\* Correspondence: skpark@kmou.ac.kr; Tel.: +82-51-410-4579; Fax: +82-51-404-3985

**Abstract:** Proton-exchange membrane fuel cells (PEMFCs) are low-temperature fuel cells that have excellent starting performance due to their low operating temperature, can respond quickly to frequent load fluctuations, and can be manufactured in small packages. Unlike existing studies that mainly used hydrogen as fuel for PEMFCs, in this study, methane is used as fuel for PEMFCs to investigate its performance and economy. Methane is a major component of natural gas, which is more economically competitive than hydrogen. In this study, methane gas is reformed by the steam reforming method and is applied to the following five gas post-treatment systems: (a) Case 1—water-gas shift only (WGS), (b) Case 2—partial oxidation reforming only (PROX), (c) Case 3—methanation only, (d) Case 4—WGS + methanation, (e) Case 5—WGS + PROX. In the evaluation, the carbon monoxide concentration in the gas did not exceed 10 ppm, and the methane component, which has a very large greenhouse effect, was not regenerated in the post-treated exhaust gas. As a result, Case 5 (WGS and PROX) is the only case that satisfied both criteria. Therefore, we propose Case 5 as an optimized post-treatment system for methane reforming gas in ship PEMFCs.

**Keywords:** fuel processing; methane reforming; post-treatment system; PEMFC; gas clean-up method



**Citation:** Bang, E.-S.; Kim, M.-H.; Park, S.-K. Options for Methane Fuel Processing in PEMFC System with Potential Maritime Applications. *Energies* **2022**, *15*, 8604. <https://doi.org/10.3390/en15228604>

Academic Editors: Eugenio Meloni, Marco Martino and Concetta Ruocco

Received: 23 September 2022

Accepted: 14 November 2022

Published: 17 November 2022

**Publisher's Note:** MDPI stays neutral with regard to jurisdictional claims in published maps and institutional affiliations.



**Copyright:** © 2022 by the authors. Licensee MDPI, Basel, Switzerland. This article is an open access article distributed under the terms and conditions of the Creative Commons Attribution (CC BY) license (<https://creativecommons.org/licenses/by/4.0/>).

## 1. Introduction

As the use of fossil fuels increases worldwide, the emissions of air pollutants and greenhouse gases generated during the combustion process also continue to increase. Therefore, to protect air quality, regulations of pollutant emissions are being tightened in many fields, including the shipping field. Various studies and experiments related to shipping fuel cells are actively being conducted as one of several methods to meet the standards required by the regulations. Research projects on existing ship fuel cells have mainly used high-temperature fuel cells, such as molten-carbonate fuel cells (MCFCs) [1] or solid oxide fuel cells (SOFCs) [2,3]. Ships such as the Viking Lady (liquefied natural gas with MCFCs) and Undine (SOFCs) of the Fellow Ship Project use these fuel cells. The efficiency of high-temperature fuel cells can be improved through cogeneration using waste heat, which has the advantage of low sensitivity to carbon monoxide (CO) compared to low-temperature fuel cells [3,4]. However, SOFCs do not start easily because of their high operating temperatures, and they respond poorly to load changes. Thus, they are not appropriate to install in ships that dock frequently or ships that sail on the coast. In contrast, proton-exchange membrane fuel cells (PEMFCs) have garnered interest as a potential power source for ships in recent years because they start easily, operate at low temperatures, respond quickly to frequent load fluctuations, and can be manufactured in a small package, making it easy to place them in a narrow space. For example, Nemo H2 and ships of the Zemships project are equipped with PEMFCs as their power sources [1]. In addition, using a method of stacking modular PEMFCs, such as those to be installed

in ZERO-V or SF-Breeze of Sandia National Laboratories, it will be possible to increase the total capacity of PEMFCs for a given amount of available space [5]. However, the aforementioned ZERO-V, SF-Breeze, Nemo H2, and ships of the Zemships project, which are already in operation, use hydrogen fuel cells. In order to use hydrogen as fuel in ships, a sufficient infrastructure to produce, store, and supply hydrogen needs to be secured. However, because hydrogen has a low density and a low boiling point, a technique for storing hydrogen in a high-pressure and low-temperature state is required to store and transport it in large amounts. However, at this point, it is very costly to construct a production, storage, and transportation facility for this purpose. Therefore, it is not very economically competitive compared to other existing fuels. For now, natural gas is the most suitable because it can be replaced with hydrogen once hydrogen is universalized as a fuel. Natural gas is highly reliable in terms of storage and transport technology, and its cost is reasonable because there is a well-established infrastructure for supplying natural gas. Due to the problems of the high price of hydrogen and its infrastructure, it is difficult to use hydrogen at this time. Therefore, in this study, unlike existing studies that mainly used SOFC stacks for ships [1–3,6] and hydrogen fuel [5], PEMFCs with methane fuel are used for ships. Methane is a raw material of PEMFC [7–13].

Methane can be converted into hydrogen by steam reforming (SR), partial oxidation reforming (POX), autothermal reforming (ATR), or anaerobic digestion (AD) [6]. The methods of SR [4,7,8,10,14–25], POX [7,8,18,23,26,27], and ATR [7–9,22,23,28,29] are used extensively. Many ships use heavy oil to reduce costs. In order to use heavy oil as fuel oil, it is essential to increase the temperature to lower the viscosity. Therefore, boilers for steam production are essential in ships that use heavy oil to increase the temperature of heavy oil. For this reason, if SR is applied to ships, the steam produced by boilers installed on existing ships can be used, and SR is widely studied as a general and traditional method [8], and the yield is the highest among several modification methods. Therefore, the steam reforming method was adopted in this study because it is easy to produce water vapor with the boiler on the ship, and steam reforming has the highest yield among several reforming methods. In this study, the steam reforming method was adopted. The methane that has passed through the reformer is converted into various types of gases, such as hydrogen, water vapor, and CO. In the case of a fuel cell system using PEMFCs, the concentration of CO in the gas that prevents poisoning of the platinum catalyst in the PEMFCs must be maintained at 10 ppm or less, but the concentration of CO in the reformed gas that has passed through the reformer exceeds 10 ppm. Therefore, a post-treatment system is required to lower the concentration of CO to an acceptable standard. For my research, a previous research work analyzed what treatment method was used as a method to process the removal of CO. Representative chemical treatment methods include water-gas shift (WGS), preference oxidation (PROX), and methanation, and previous papers mentioned the use of the following combinations. In the case of Refs. [7,9,11,13,14,30], a combination of water-gas shift (WGS) and preference oxidization (PROX) was applied; in other studies [7,15,30–32], WGS and methanation reactor were used; in yet others, a physical method, pressure swing adsorption (PSA), was mentioned [7,10]. In the case of Ref. [7], a method for producing pure hydrogens, such as PSA, PROX, and methanation, including WGS, was mentioned in a study on the production of hydrogen during steam reforming of methane based on a membrane reactor. Ref. [9] compared the performance of a fuel processor using WGS and PROX with a change in WGS position in the membrane unit to provide an effective fuel processor for the methane autothermal reforming PEMFC system. Ref. [11] studied glycerol steam reforming for optimum hydrogen production conditions of low-temperature PEMFCs (LT-PEMFCs) and high-temperature PEMFCs (HT-PEMFCs), and WGS and PROX were used together as a fuel processor for LT-PEMFCs. Ref. [13] modeled a system that executes WGS and PROX with a methane autothermal simulation. Ref. [33] modeled and tested the case of using WGS (second stage of high-temperature WGS, or HTS; the first stage of low-temperature WGS, or LTS) and second-stage PROX as a methane fuel processing system. Ref. [18] studied the CO removal effect depending on the

PROX catalyst (Pt, Ru, Co, Fe) for PEMFCs. Ref. [33] studied a Ni catalyst to improve WGS and methanation reaction for CO removal and mentioned that the methanation reaction can replace PROX, which requires oxygen. Refs. [15,30,32] analyzed the case of using WGS and a methanation reactor to purify methane-modified mixed gas. In Ref. [7], WGS and PROX, PSA physical CO removal methods were used to remove CO. Ref. [10] collected a hydrogen stream for a CO<sub>x</sub>-free method using a Pd-based membrane reactor (MR).

As described above, the previous studies used only one or two methods for removing CO in the reformed methane for simulation or experiment, and the rest of the methods were only mentioned. Therefore, in this study, in addition to the fuel treatment methods (or post-treatment systems) used in the previous studies, various combinations of post-treatment methods are compared and analyzed to determine which fuel treatment system is suitable for application in fuel-efficient PEMFC systems in ships. In this paper, five systems—(a) WGS only, (b) methanation only, (c) PROX only, (d) WGS + methanation (e), and WGS + PROX—are designed using Matlab Simulink and Thermolib [34]. Based on the results of calculation and analysis of the composition and molar flow rate, the goal of the study is to propose a PEMFC system for ships that uses fuel-efficient and optimal methane for PEMFC systems as a power source.

## 2. Methodology

### 2.1. Modeling

A fuel cell system that uses non-hydrogen fuel utilizes the process presented in Figure 1. First, the methane is supplied. Second, the methane is converted into hydrogen (the gas production section). Third, the changed gas is purified in the gas post-treatment process (the gas clean-up section), and finally, the purified gas is supplied to the fuel cell stack.



Figure 1. Schematic of methane reforming PEMFC system.

Figure 2 shows the supply unit of methane gas to the gas clean-up section for the reformed gas treatment. In the case of the gas clean-up section, the combination to be applied in this study is shown in the figure.

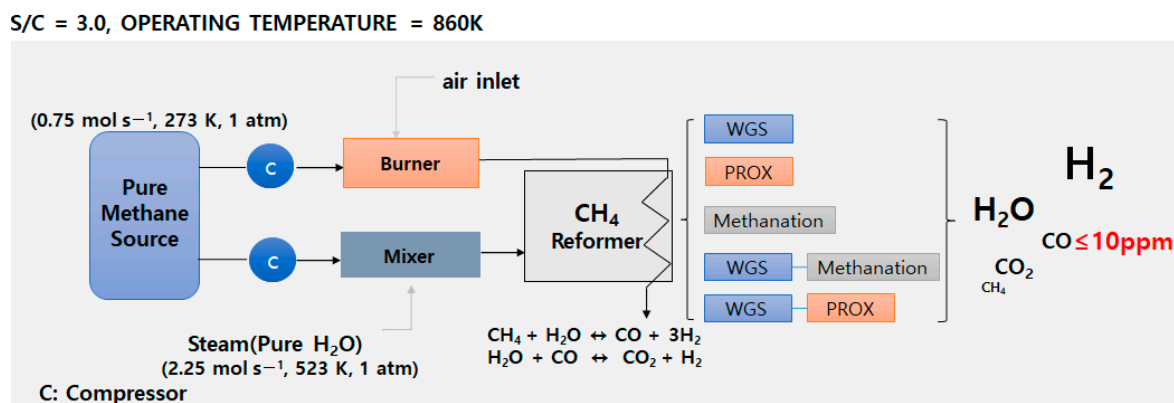
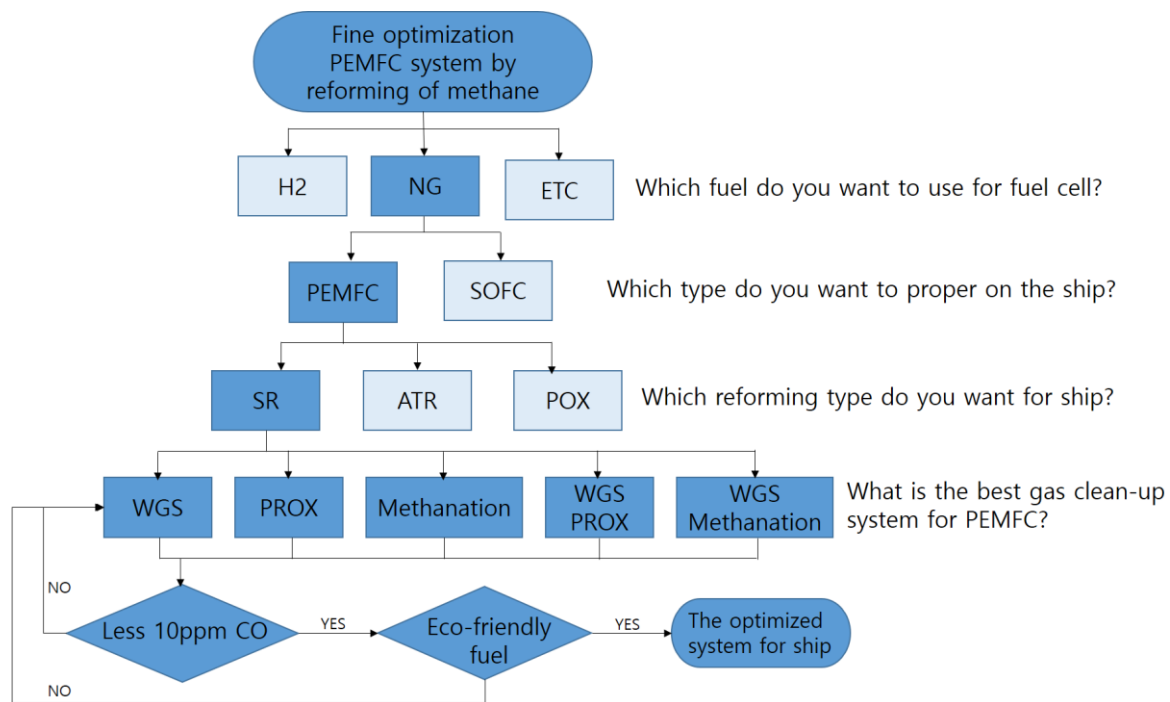


Figure 2. Schematic of methane reforming system.

In this study, the system that was constructed is shown in Figure 2, and the research was conducted using the method shown in Figure 3. The feed fuel was methane, and the fuel cell stack contained PEMFCs. The SR method was used as the reform method, and the methane and water vapor were supplied at a rate of S/C = 3.0 (S/C is the steam-to-

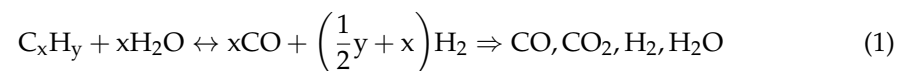
carbon ratio). In this study, as shown in Figures 2 and 3, the calculated results obtained by applying five different combinations of WGS, methanation, and PROX as the gas post-treatment process are evaluated according to the following conditions: (1) whether the CO concentration satisfies the standard and (2) whether the fuel cell system emphasizes fuel efficiency (minimal greenhouse gas emissions). Considering these conditions, we propose an optimized gas post-treatment system for PEMFCs in ships using methane fuel. For the simulation, a reforming system and a post-treatment system were constructed using Matlab Simulink and Thermolib [34].



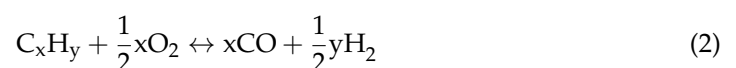
**Figure 3.** Process of methane reforming PEMFC system.

## 2.2. Reforming Methods

The reforming methods introduced in this study are as follows: (1) SR, (2) POX, and (3) autothermal reforming (ATR). First, in the SR method, when the hydrocarbon fuel is mixed with water vapor in the presence of a catalyst at a high temperature, an endothermic reaction, as shown in the equation below, occurs [35].

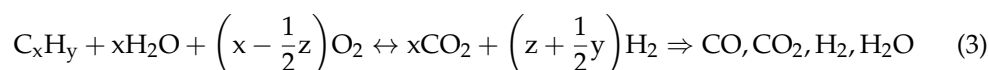


For all reforming methods, except for the SR method, oxygen ( $O_2$ ) is required for reforming; thus, the air is supplied. At this time, because nitrogen ( $N_2$ ), which comprises 79% of the air, is also supplied, the exhaust gas at the outlet side of the reformer is diluted with nitrogen to lower the proportion of hydrogen in the outlet gas. On the other hand, the SR method has the highest yield among several reforming methods because oxygen ( $O_2$ ) produced by using moisture ( $H_2O$ ) is not required during the reaction. Second, in the case of POX, a reforming method that uses a partial oxidation reaction of hydrocarbon fuel and oxygen as an exothermic reaction to convert the fuel into a mixed gas of CO and hydrogen proceeds under a catalytic reaction. It has the same reaction formula as Equation (2) [35]:



Because oxygen is required for the reaction, the outlet gas is diluted with nitrogen, which is supplied with oxygen from the air, giving it the lowest hydrogen yield of the three

reforming methods. Lastly, the ATR combines SR, POX, and water–gas conversion. It has the same reaction formula as Equation (3). The ATR method proceeds in the same reactor and receives its heat supply for the endothermic steam reforming reaction and water–gas conversion reaction through a partial oxidation reforming reaction. In the ATR, steam is used as a reactant, and therefore, steam reforming is included. Partial oxidation reforming is also used because less oxygen is used than the stoichiometric amount of oxygen [35]:



Because there is a boiler on the ship, it is easy to supply steam, giving SR the highest yield among several reforming methods. In the case of steam reforming of methane, both the reforming reaction of Equation (4) and the shift reaction of Equation (5) occur simultaneously [35,36].

(1) Reforming Reaction



$$(\Delta H^\circ = +206.4 \text{ kJ mol}^{-1})$$

(2) Shift Reaction



$$(\Delta H^\circ = -41.2 \text{ kJ mol}^{-1})$$

Because the reforming reaction is an endothermic reaction, and the shift reaction is a weak exothermic reaction, the overall reaction combining the two reactions is an endothermic reaction.

Therefore, the heat source for the reforming reaction is supplied to the reformer through the burner. Because the endothermic reaction of steam reforming occurs inside the tube, a portion of the fuel is usually used to heat the tube. In the case of high-temperature fuel cell systems, such as SOFCs and MCFCs, the reformer tube is also heated by using the exhaust gas from the fuel cell stack outlet. A reforming system for a fuel cell aims to reform a hydrocarbon-type fuel to produce a final product with the lowest impurities and the highest hydrogen content. In the steam-reformed methane, CO is produced according to the reforming equation. The platinum (Pt) catalyst in PEMFCs is vulnerable to CO and causes poisoning. To prevent this, the CO concentration in the reformed gas must be maintained at 10 ppm or less [35–38]. Because this study was conceived as a marine system, the steam reforming method, for which it is easy to secure steam, was applied.

### 2.3. Post-Treatment System

There are three types of post-treatment systems applied in this study: (1) water–gas shift reaction (WGS reaction), (2) selective methanation of CO, and (3) selective oxidation of CO (or PROX). Hydrogen can be additionally generated through the secondary reaction of CO discharged from the outlet of the reformer. This process is called the water–gas shift reaction (WGS) [35]. WGS serves to increase the hydrogen yield in the reformed gas and lower the CO yield by converting CO in the reformed gas to hydrogen and carbon dioxide (CO<sub>2</sub>) through the reaction with water vapor. The CO yield is defined as the molar ratio of CO to the reformed gas [35]:

$$y_{CO} = \frac{n_{CO}}{n} \quad (6)$$

Here,  $n_{CO}$  is the number of moles of CO in the reformed gas, and  $n$  is the total number of moles of the reformed gas. The water–gas conversion reaction generally reduces the CO

yield under the catalyst by 0.2~1.0% [36]. When water vapor and CO react in WGS, a weak exothermic reaction occurs, as demonstrated by the following chemical formula:



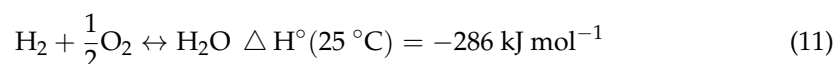
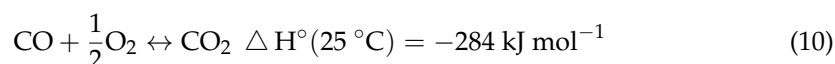
Because this is an exothermic reaction, the water–gas conversion reaction (according to Le Chatelier’s law) increases the equilibrium in the direction of the reactant at high temperatures, which increases CO and moisture but decreases the hydrogen yield. The reaction has a high hydrogen yield at low temperature, but the reaction rate is high at a high temperature. Thus, the water–gas converter is separated into two stages for a high hydrogen yield and a fast reaction rate. These stages are called low-temperature WGS (LTS) and high-temperature WGS (HTS); they use HTS to rapidly react at high temperature and increase yield using LTS [36]. WGS utilizes LTS and HTS and increases the yield of hydrogen at LTS (operating temperature 150–250 °C under the catalyst) and increases the reaction rate at HTS (operating temperature 400–500 °C under the catalyst) [35].

The purpose of this study was to increase the hydrogen yield of WGS and to reduce the yield of CO. Therefore, it was simulated using integrated WGS in the temperature range of LTS. When the water–gas converter is used alone, it is difficult to satisfy the conventional CO tolerance of 10 ppm or less, and thus, a process for removing CO is required. There is a method using a chemical reaction and a method using physical separation. In this study, the method for removing CO using a chemical reaction was applied, not the pressure separation adsorption method or the physical separation method using palladium membrane separation. The first chemical method for CO removal is the use of selective methanation of CO (methanation). Because the reformed gas contains both CO and CO<sub>2</sub>, when the gas reacts with hydrogen, the reactions described by the following two formulae occur simultaneously in methanation [36]:



Therefore, because the amount of hydrogen consumed to remove CO was large, it was usually used when the concentration of CO in the reforming gas was low. To remove 1 mol of CO, 3 mols of hydrogen was consumed, and CO<sub>2</sub> was also methanized by consuming 4 mols of hydrogen. Because this reaction does not require oxygen, there is no need to supply air. However, a large amount of hydrogen is required to remove CO, and it produces methane (a greenhouse gas) as a result of the reaction. Nevertheless, this is a suitable method when the fraction of CO in the reformed gas is small [35].

Another method for removing CO is selective oxidation of CO (or PROX). The concentration of CO can be reduced by converting CO to CO<sub>2</sub> through a reaction with oxygen in the air. The two response formulae are [35]



Equation (10) reduces the yield of CO, but Equation (11) reduces the yield of hydrogen. Thus, the catalyst can be used to promote the reaction of Equation (10) and suppress the reaction of Equation (11). In addition, PROX requires a supply of air to be oxidized in order to remove CO, and nitrogen flows in during this process to decrease the hydrogen yield.

The above reaction is influenced by selectivity and efficiency. Selectivity affects the amount of total oxygen consumption required for CO removal, and efficiency affects the

degree to which CO is oxidized and converted. During this process, hydrogen is also oxidized, the degree of which is determined according to the following equation [35]:

$$\eta(1 - S) \quad (12)$$

where  $S$  is the selectivity, and  $\eta$  is the efficiency. Their values depend on the performance of the catalyst or PROX and are affected by temperature.

### 3. Results

#### 3.1. Reforming

For the simulation of the post-treatment system, a methane steam reforming system was designed using Matlab Simulink and Thermolib [34]. The operating conditions of the steam reforming system for calculating the reformed gas results are shown in Table 1. At a pressure of 1 atm,  $0.25 \text{ mol s}^{-1}$  of methane and  $0.75 \text{ mol s}^{-1}$  of water vapor were constantly supplied at  $S/C = 3.0$ . The supplied methane and steam were reformed at a reformer operating temperature of 860 K. Table 1 shows the results obtained by simulating and calculating the methane steam reforming system obtained based on these conditions and designs.

**Table 1.** Results for the reformer outlet side.

Outlet Temp. [K]	Molar flow [ $\text{mol s}^{-1}$ ]				Molar Fraction				
	Outlet	H <sub>2</sub>	Methane Used	CO	H <sub>2</sub>	Methane	H <sub>2</sub> O	CO	CO <sub>2</sub>
860.30	4.48	2.62416	0.73959	0.33418	0.58612	0.00188	0.24681	0.07464	0.09055

Based on this, we simulated five methane reforming gas post-treatment systems in this study: (1) Case 1—WGS only, (2) Case 2—methanation only, (3) Case 3—PROX only, (4) Case 4—WGS + methanation, (5) Case 5—WGS + PROX. The optimization system was selected by comparing the gas composition ratio, and the molar flow rate was selected by comparing the results before and after the simulation of the post-treatment system.

#### 3.2. Post-Treatment System

##### 3.2.1. Case 1: WGS Only

Matlab Simulink was used to construct the system, the schematic of which is shown in Figure 4a. In Figure 4a, 1 meant the gas production section and 2 meant the gas clean-up section. Figure 4 also shows a graph of the temperature dependence of the results for the outlet of the WGS system. Figure 4b shows the molar flow, and Figure 4c shows the molar fraction. As a result of increasing the temperature in 20 K increments from 420 K to 580 K, the WGS reaction increased the CO and moisture as the equilibrium tilted toward the reactant at high temperatures. However, the hydrogen yield decreased; the lower the temperature, the higher the hydrogen flow rate and fraction. In addition, the flow rate and fraction of CO decreased. According to Le Chatelier's law, when the pressure of the system increases, the reaction occurs in the direction of the decreasing pressure. Therefore, as the pressure of the supplied fuel and water vapor increased, the amount of hydrogen production decreased. Therefore, the lower the pressure of the supplied fuel and water vapor, the higher the outlet flow rate and the hydrogen flow rate. In order to be used for PEMFCs, the molar fraction of CO in the outlet gas should not exceed 0.00001, but as shown in Figure 4, WGS alone is not suitable for PEMFCs because of the molar concentration of CO.

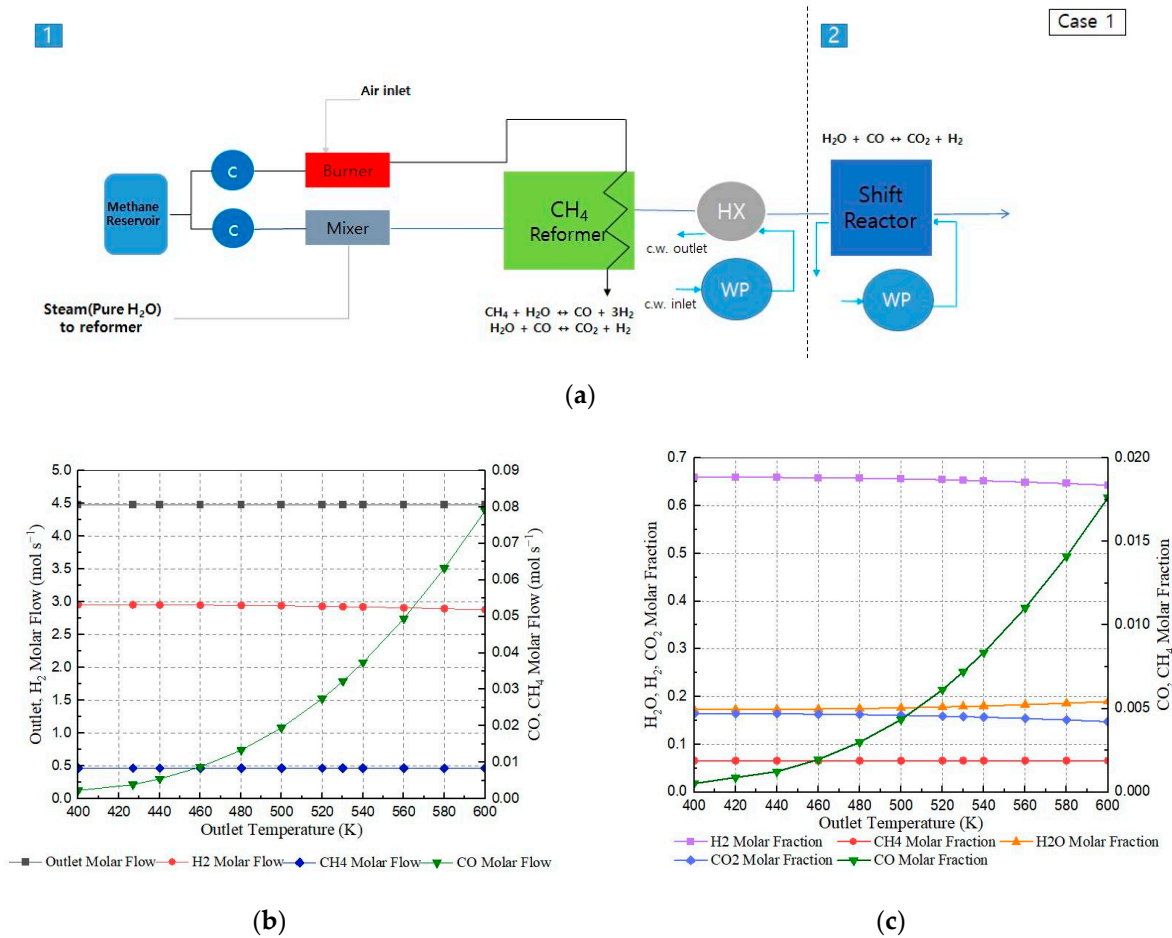


**Figure 4.** (a) Schematic of methane reforming system for PEMFCs, Graph of (b) molar flow and (c) molar fraction of outlet side (Case 1).

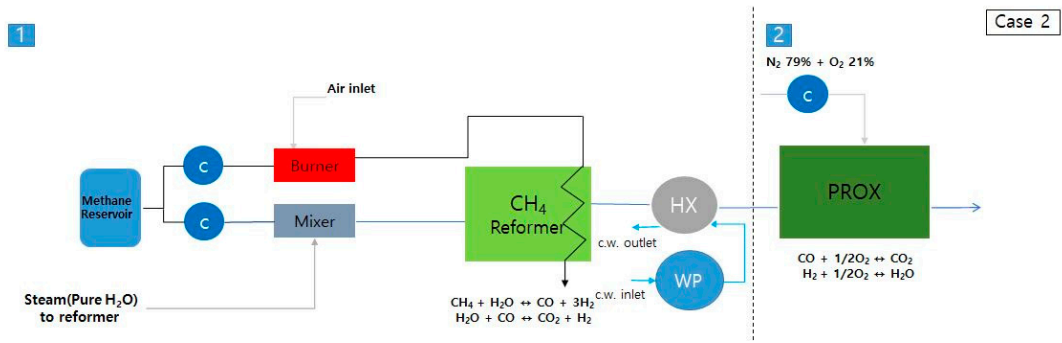
3.2.2. Case 2: PROX Only

The second case is where PROX is applied as a reactor for removing CO through a selective oxidation catalyst. Figure 5a shows a schematic diagram of the system in which PROX is applied.

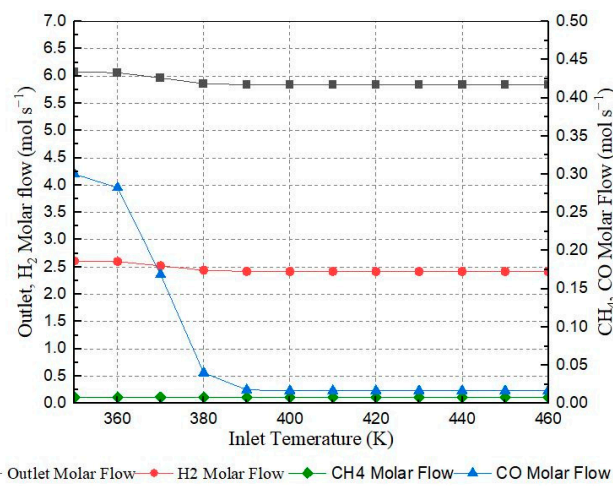
In this system, the change of selectivity and efficiency according to the temperature is reflected using the look-up tables, which are shown in Tables 2 and 3. Table 2 shows the efficiency value according to the PROX inlet temperature and the change in the CO molar fraction. As the temperature increases, the efficiency of PROX increases, thereby decreasing the molar fraction of CO on the outlet side of PROX.

**Table 2.** PROX efficiency according to inlet temperature.

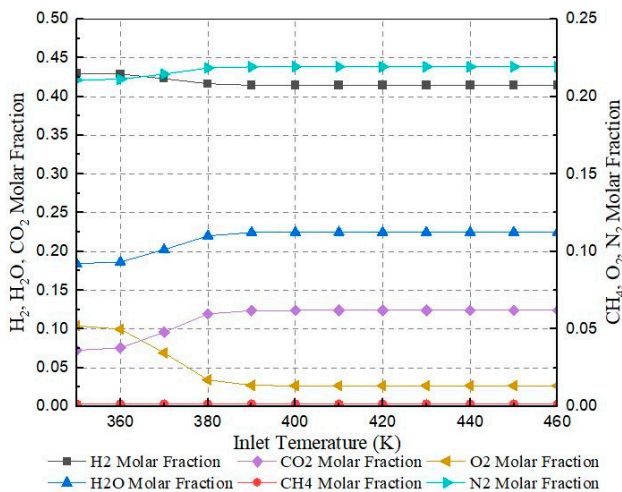
Inlet Temp. [K]	Value	After Reformer CO Fraction	After PROX CO Fraction
323	0	0.074642219	0.063159
393	0.1		0.057105
403	0.5		0.054042
413	0.5		0.032221
423	0.9		0.006519
433	0.95		0.003263



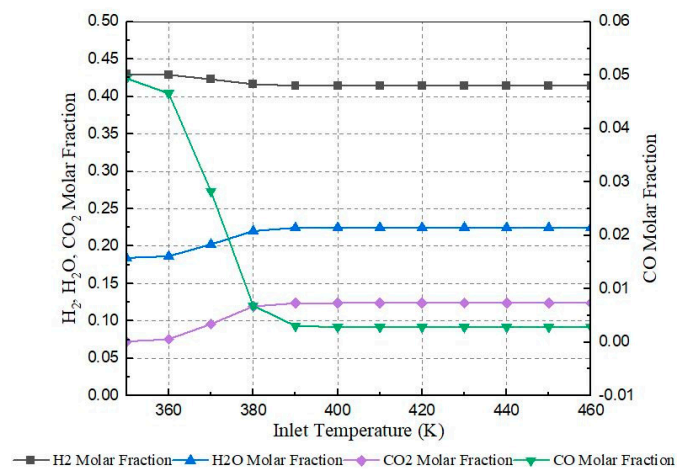
(a)



(b)



(c1)



(c2)

Figure 5. Schematic of (a) Case 2 reforming system and Graph of (b) molar flow and (c1,c2) molar fraction of outlet side.

**Table 3.** PROX selectivity according to inlet temperature.

Inlet Temp. [K]	Value	After Reformer H <sub>2</sub> Fraction	After PROX H <sub>2</sub> Fraction	After Reformer O <sub>2</sub> Fraction	After PROX O <sub>2</sub> Fraction	After Reformer CO Fraction	After PROX CO Fraction
323	0.9	0.5861222	0.511425	0.0321567	0.0019884	0.0746422	0.0032591
393	0.8		0.511114		0.0017801		0.0032598
403	0.75		0.510959		0.0016759		0.0032601
413	0.6		0.510492		0.0013631		0.0032611
423	0.45		0.510025		0.0010501		0.0032622
433	0.4		0.509870		0.0009457		0.0032625

Efficiency value = 0.95.

Table 3 shows the change in selectivity with temperature. As mentioned above, selectivity affects the degree of total oxygen consumption required for CO removal. Thus, the oxygen consumption rate increases as selectivity decreases. When  $S = 1$ , hydrogen is not oxidized. Therefore, in order to minimize the consumption rate of hydrogen for good output, the value of selectivity should be kept as close to 1 as possible.

Table 4 shows how the molar fraction of hydrogen changes according to Equation (12) when the inlet temperature of PROX changes. The molar fraction of hydrogen depends on selectivity and efficiency. Furthermore, as the inlet temperature of PROX increases, the value of selectivity decreases, and the value of efficiency increases.

**Table 4.** Fraction of hydrogen according to  $\eta(1 - S)$ .

Inlet Temp. [K]	Selectivity Value	Efficiency Value	After Reformer H <sub>2</sub> Fraction	After PROX H <sub>2</sub> Fraction
323	0.9	0	0.586122238	0.49638
393	0.8	0.1		0.49707
403	0.75	0.5		0.497182
413	0.6	0.5		0.499353
423	0.45	0.9		0.508082
433	0.4	0.95		0.50987

Figure 5b graphically shows the calculation results of the gas flow rate and distribution at the outlet side according to the PROX inlet temperature, to which the selectivity and efficiency values shown in Table 4 were applied. Figure 5(c1,c2) show the temperature dependence of the results. Figure 5a is the value of the molar flow rate, and Figure 5b is the value of the molar fraction. Depending on the value of efficiency, the molar flow rate and the molar fraction of CO processed through PROX are different. The efficiency increased as the temperature increased, but it had a constant efficiency value above 433 K. Calculating the efficiency of 99.9%, assuming PROX with ideal efficiency, the fraction of CO could drop to 0.002, but it did not satisfy 10 ppm. In addition, when PROX was used, the reaction of oxidizing CO and oxidizing hydrogen occurred simultaneously, and the air for oxidizing them was additionally supplied. Therefore, the molar fraction of hydrogen was smaller than when using WGS alone. The molar fraction of CO sharply decreased from 350 K to 390 K at the inlet temperature but exceeded 0.00001. Thus, the gas that had been post-treated with reformed gas only was not suitable for PEMFCs. The PROX used in this calculation was based on a typical degree of efficiency and selectivity, and the degree of oxidation and hydrogen oxidation of CO may vary according to the efficiency and selectivity, depending on the inlet temperature or its own performance.

### 3.2.3. Case 3: Methanation Only

The third case is where a methanation reactor is installed to remove CO through selective CO methanation. Figure 6a shows the schematic of the system in which PROX is applied as a gas post-treatment. Figure 6 also shows the results calculated by passing the methanation reactor through a gas post-treatment. Figure 6b is the molar flow rate, and Figure 6c shows the calculation result for the molar fraction. When comparing the hydrogen flow rate and the molar fraction, it was confirmed by numerical value that the hydrogen yield was significantly lower than that when using WGS or PROX alone. When using WGS or PROX, the hydrogen flow exceeded  $2.0 \text{ mol s}^{-1}$ , whereas in the case of methanation alone, it did not reach  $2.0 \text{ mol s}^{-1}$ . In addition to this, even when the operating temperature was increased, the hydrogen yield did not increase significantly, and the molar fraction of CO exceeded 10 ppm when it was 590 K or more, which did not satisfy the standard. Accordingly, the methanation reactor was effective in removing a small amount of CO, and the lower the operating temperature, the lower the molar fraction of CO. If the methanation reactor was used alone, the concentration of CO may have been below the standard, but the sole use of the methanation reactor was not appropriate because the hydrogen consumption rate for removing CO was high, and the hydrogen yield was significantly lower.

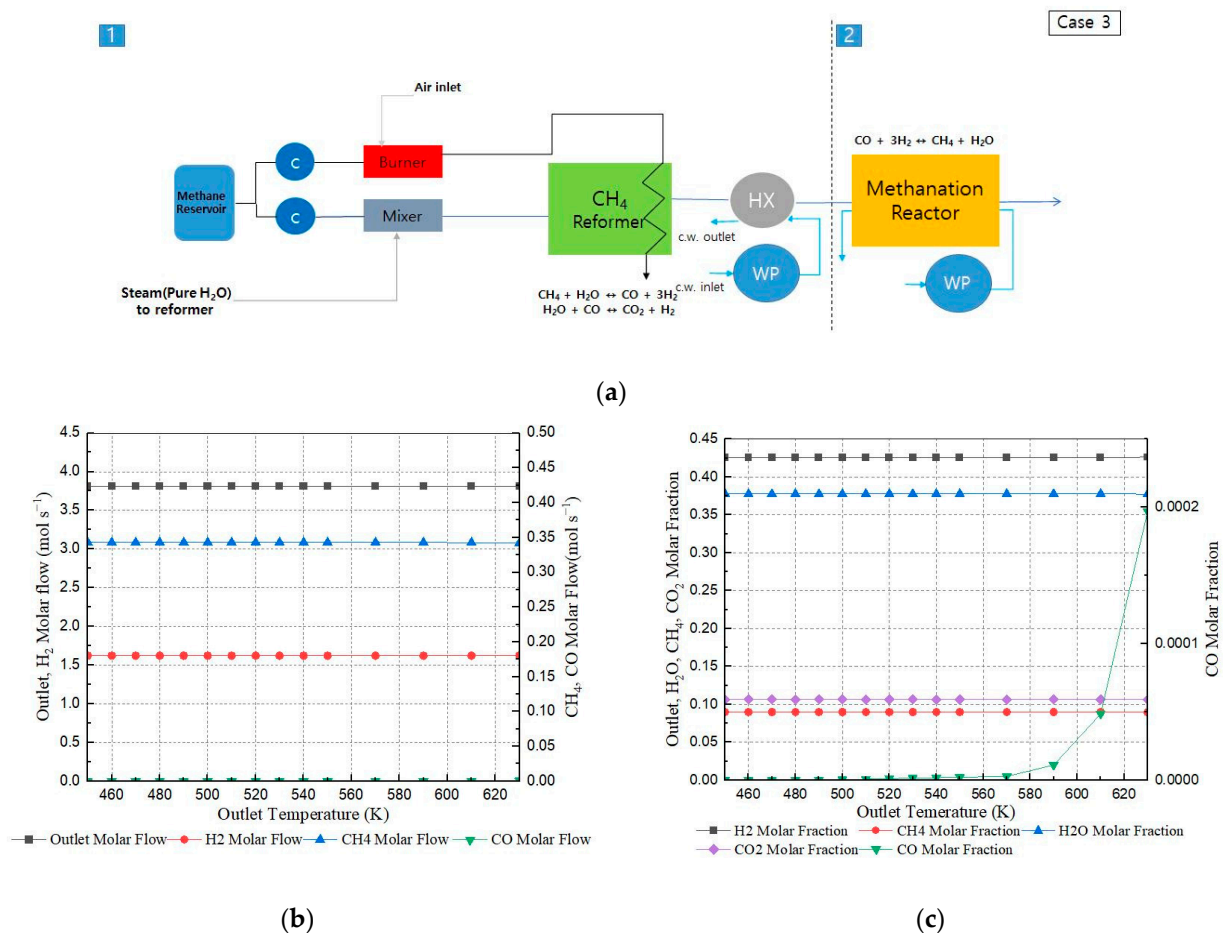


**Figure 6.** Schematic of (a) Case 3 reforming system and Graph of (b) molar flow and (c) molar fraction of outlet side.

### 3.2.4. Case 4: WGS + Methanation

Case 4 and Case 5 were calculated by combining two types of post-treatment (WGS and methanation), and additional post-treatment systems were installed based on WGS. Figure 7 displays the setup for Case 4; the system simultaneously applies WGS and methanation, and an additional methanation reactor is installed in WGS. Table 5 shows the results of the

gas passing through the WGS reactor. As shown in Table 5, when only WGS is applied, the molar fraction of CO is 0.003. Thus, to lower it below 0.00001, a methanation reactor was added as the next step of WGS. Table 6 shows the results when the WGS and methanation reactor are applied simultaneously. The results indicate that the molar fraction of CO was greatly reduced and dropped to zero. The molar fraction of hydrogen was also excellent in terms of output, with a high value significantly exceeding  $2.0 \text{ mol s}^{-1}$ . This is much higher than that of Case 3, which applied only the methanation reactor alone. Through the water–gas conversion reaction of WGS, the hydrogen flow rate, which was  $2.6 \text{ mol s}^{-1}$  at the outlet side of the reformer, was increased to  $2.9 \text{ mol s}^{-1}$ . Furthermore, the CO tolerance standard of 10 ppm or less was met through the methanation reactor, and methane was produced. The greenhouse effect of one molecule of methane is 21 times that of  $\text{CO}_2$ , and it is also an air pollutant. Therefore, it was not suitable as a fuel cell system that values fuel efficiency and minimizes pollution, making it necessary to reconsider the application of the methanation reactor.

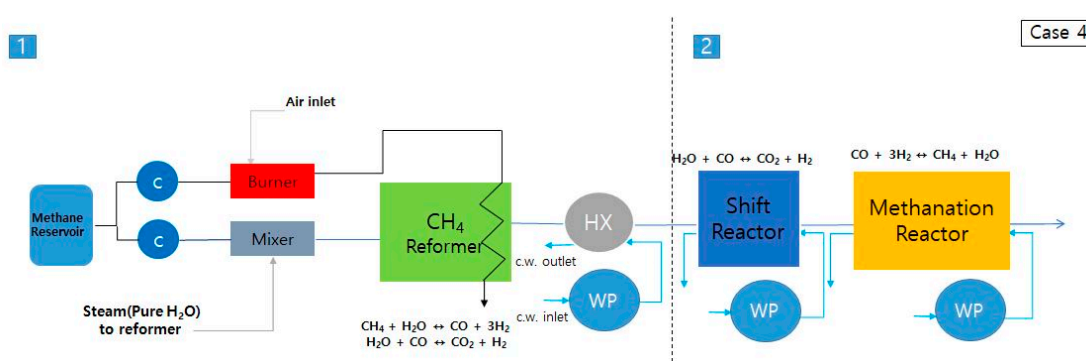


Figure 7. Schematic of Case 4 reforming system.

Table 5. Results for WGS outlet side.

Outlet Temp. [K]	Molar Flow [ $\text{mol s}^{-1}$ ]				Molar Fraction				
	Outlet	$\text{H}_2$	Methane	CO	$\text{H}_2$	Methane	$\text{H}_2\text{O}$	CO	$\text{CO}_2$
480.68	4.480	2.947	0.008	0.013	0.658	0.002	0.175	0.003	0.162

Table 6. Results for (WGS + methanation reactor) outlet side.

Outlet Temp. [K]	Molar Flow [ $\text{mol s}^{-1}$ ]				Molar Fraction				
	Outlet	$\text{H}_2$	Methane	CO	$\text{H}_2$	Methane	$\text{H}_2\text{O}$	CO	$\text{CO}_2$
499.75	4.453	2.906	0.022	0	0.653	0.005	0.179	0	0.163

### 3.2.5. Case 5: WGS + PROX

Figure 8 demonstrates Case 5, showing a system that installed additional PROX on WGS. The results shown in Table 7 demonstrate that by installing PROX, the hydrogen yield is increased, and the concentration of CO is further reduced through WGS. When the WGS and PROX reactors were applied at the same time, the hydrogen flow rate was increased by the water–gas conversion reaction of WGS at the outlet side of the reformer, and the CO concentration of the PEMFCs dropped below the reference value by oxidizing and removing CO from PROX. As mentioned before, the amount of oxygen and the conversion required for the oxidation reaction of CO are affected by selectivity (S) and efficiency ( $\eta$ ). These variables change the performance of PROX, depending on the temperature, catalyst, or material at the inlet side of PROX. The flow of hydrogen and CO at the outlet side of PROX may be changed due to their influence.

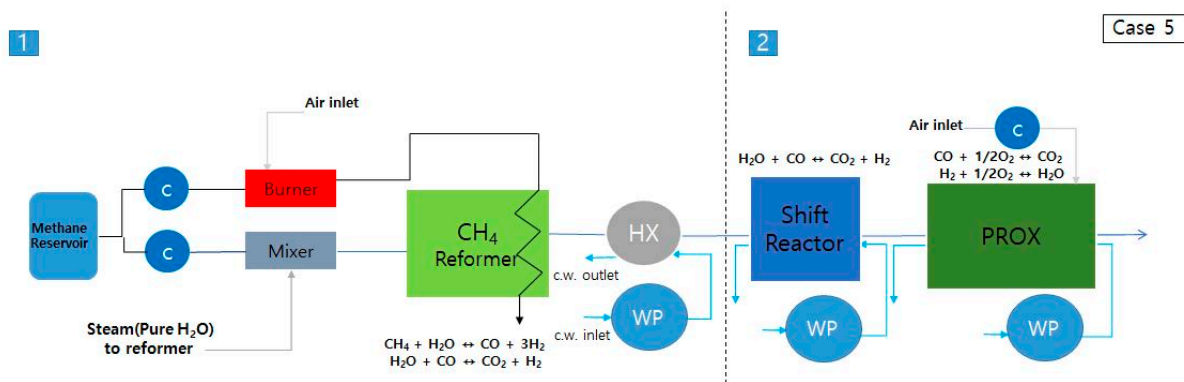


Figure 8. Schematic of Case 5 reforming system.

Table 7. Results for (WGS + PROX reactor) outlet side.

Outlet Temp. [K]	Molar Flow [ $\text{mol s}^{-1}$ ]						Molar Fraction					
	Outlet	H <sub>2</sub>	Methane	CO	H <sub>2</sub>	Methane	H <sub>2</sub> O	CO	CO <sub>2</sub>	O <sub>2</sub>	N <sub>2</sub>	
443.57	5.566	2.642	0.008	$4.05 \times 10^{-5}$	0.475	0.002	0.196	$7.27 \times 10^{-6}$	0.133	0.018	0.177	

### 3.3. Results Analysis

Table 8 shows the results of the calculation of the molar flow rate and molar fraction at the outlet side of each post-treatment system according to the components.

Table 8. Overall results.

	Molar Flow [ $\text{mol s}^{-1}$ ]						Molar Fraction					
	Outlet	H <sub>2</sub>	Methane	CO	H <sub>2</sub>	Methane	H <sub>2</sub> O	CO	CO <sub>2</sub>	O <sub>2</sub>	N <sub>2</sub>	
WGS (Case 1)	4.480	2.947	0.008	0.013	0.658	0.002	0.175	0.003	0.162	-	-	
PROX (Case 2)	5.838	2.419	0.008	0.017	0.414	0.001	0.225	0.003	0.124	0.013	0.219	
Methanation (Case 3)	3.811	1.623	0.343	0	0.426	0.090	0.378	0	0.106	-	-	
WGS + Methanation (Case 4)	4.453	2.906	0.022	0	0.653	0.005	0.179	0	0.163	-	-	
WGS + PROX (Case 5)	5.566	2.642	0.008	$4.05 \times 10^{-5}$	0.475	0.002	0.196	$7.27 \times 10^{-6}$	0.133	0.018	0.177	

To prevent the poisoning of the platinum catalyst in the PEMFCs, the concentration of CO in the reformed gas that has passed through the post-treatment system should not exceed 10 ppm. In addition, the fuel cells are fuel-efficient power sources that produce minimal emissions, and the systems for fuel cells should not support an increase in air pollutants. Although there are various types of greenhouse gases, the greenhouse effect of one molecule of methane is 21 times that of one molecule of CO<sub>2</sub>. Therefore, methane regenerated as a result of a post-treatment system would defeat the purpose of the system. In the case of CO<sub>2</sub>, another greenhouse gas, as shown in Table 8, the ratio of CO<sub>2</sub> in the exhaust gas is 0.163 at the maximum and 0.106 at the minimum. The difference between the five cases is small, but in the case of methane, the difference in the molar fraction is from the maximum of 0.09 to the minimum of 0.001. As it shows a large difference of about 90 times, the effect of methane is considered to be greater in terms of both the greenhouse effect and the ratio, so only methane excluding CO<sub>2</sub> was evaluated in the eco-friendliness evaluation.

Table 9 compares the results of each post-treatment system in terms of two evaluation factors: whether it satisfies the standard concentration of CO and eco-friendliness. If methane is regenerated, the system is considered not to be environmentally friendly.

**Table 9.** Scores for each case.

Type of Post-Treatment System	Satisfaction of CO Standard Concentration ( $\leq 10$ ppm)	Eco-Friendly (Methane Regeneration)
WGS (Case 1)	Bad	Good
PROX (Case 2)	Bad	Good
Methanation (Case 3)	Good	Bad
WGS + Methanation (Case 4)	Good	Bad
WGS + PROX (Case 5)	Good	Good

The post-treatment system combining WGS + PROX is the most desirable because it is the only post-treatment system that satisfies the reference concentration of CO and does not produce methane, a greenhouse gas, as a result of the reaction.

#### 4. Discussion

This study aimed to find the most optimized methane gas treatment system by utilizing a methane reforming PEMFC system with marine fuel cell systems. The current systems discharge methane, which has a high impact on global warming, through a gas treatment system and maintain as much of the hydrogen generated during the reforming process as possible. As a result of the calculations using Matlab Simulink, it was concluded that Case 5 (WGS + PROX) is the most appropriate in the scope of this study. However, if the results of only the hydrogen aspect are observed, the program calculation results show that Case 4 (WGS + methanation) has a greater molar amount of hydrogen than Case 5 (WGS + PROX). Therefore, Case 4 (WGS + methanation) can be a more optimal method in some cases. However, at present, the limiting criteria for methane emissions are not clear, and thus, we concluded that Case 5 (WGS + PROX) is a more optimized system than Case 4 (WGS + methanation), which regenerates and discharges methane. The results of an experiment with the same specimen are necessary, and in the case of the empirical study, it seems necessary to apply both low temperature and high temperature to the case of WGS to model and apply it to suit the system. In addition, because this study conceived a methane reforming PEMFC system limited to a marine fuel cell system, only the case of SR reforming was dealt with in consideration of ships with abundant water vapor supply. However, in future studies, it would be better to add a study comparing the calculated results by applying both the ATR method and the POX method to reforming methane, as well as the SR method. It would be better if research were conducted in parallel. Additionally, in this study, the environmental performance was evaluated based on methane emissions, which has the greatest greenhouse effect among the greenhouse gases that cause global warming. It is necessary to consider more types of reference substances.

#### 5. Conclusions

In this study, a method of applying PEMFCs as a power source for ships was proposed. The goal was to propose an optimized gas treatment method by comparing the simulated calculation results of passing the reformed gas through a post-treatment system, for which five designs were simulated using Matlab Simulink. At a pressure of 1 atm,  $0.25 \text{ mol s}^{-1}$  of methane and  $0.75 \text{ mol s}^{-1}$  of water vapor were constantly supplied at  $S/C = 3.0$ . Methane gas was reformed and supplied to the gas treatment system under constant conditions of 860 K. The five cases were: Case 1—WGS only, Case 2—PROX only, Case 3—methanation only, Case 4—WGS + methanation, and Case 5—WGS + PROX. Each of the five gas handlers passed through the calculation result in the supply gas to prevent the Pt poisoning

phenomenon in the PEMFCs. Each system was evaluated for its eco-friendliness based on whether or not the CO concentration was less than 10 ppm and whether methane gas was regenerated. As a result of evaluating the systems according to the standard evaluation factors (CO concentration, system eco-friendliness), Case 5 (WGS + PROX) was the only one to satisfy both criteria. Therefore, we propose Case 5 (WGS + PROX) as an optimized post-treatment method for gas. However, for Case 4 (WGS + methanation), if the amount of methane generated as a result of applying Case 4 does not exceed the allowable value, it may be considered suitable as a PEMFC system. However, at present, there is no clear emission standard regarding methane emission. Case 4 may also be suitable for PEMFC systems, provided there is a device that transports the recovered methane back to the feed gas section. However, in this study, only the suitability was judged by analyzing only the gas component of the exhaust gas because the device was not applied to the research content. Therefore, we conclude that Case 5 (WGS + PROX) is the most suitable reformed gas post-treatment system for ship methane fuel reforming PEMFCs.

**Author Contributions:** Conceptualization, E.-S.B.; Methodology, M.-H.K.; Software, E.-S.B.; Validation, M.-H.K.; Writing—original draft, E.-S.B.; Visualization, E.-S.B.; Supervision, S.-K.P. All authors have read and agreed to the published version of the manuscript.

**Funding:** This research received no external funding.

**Acknowledgments:** This research did not receive any specific grant from funding agencies in the public, commercial, or not-for-profit sectors. This thesis was reconstructed using data from Eun-Shin Bang's 2020 master thesis.

**Conflicts of Interest:** There are no conflicts of interest to declare.

## References

1. Tronstad, T.; Astrand, H.H.; Haugom, G.P.; Langfeldt, L. *Study on the Use of Fuel Cells in Shipping*; European Maritime Safety Agency: Lisbon, Portugal, 2017.
2. Van Biert, L.; Godjevac, M.; Visser, K.; Aravind, P.V. A review of fuel cell systems for maritime applications. *J. Power Sources* **2016**, *327*, 345–364. [[CrossRef](#)]
3. Kim, M.-H. Performance and Safety Analysis of Marine Solid Oxide Fuel Cell and Gas Turbine Hybrid Power System (under Conditions of Turbine Cooling and Constant TIT). *J. Korean Soc. Mar. Eng.* **2009**, *33*, 484–496.
4. Liso, V.; Olesen, A.C.; Nielsen, M.P.; Kær, S.K. Performance comparison between partial oxidation and methane steam reforming processes for solid oxide fuel cell (SOFC) micro combined heat and power (CHP) system. *Energy* **2011**, *36*, 4216–4226. [[CrossRef](#)]
5. Klebanoff, L.E.; Pratt, J.W.; Madsen, R.T.; Caughlan, S.A.M.; Leach, T.S.; Appelgate, T.B., Jr.; Kelety, S.Z.; Wintervoll, H.-C.; Haugom, G.P.; Teo, A.T.Y.; et al. *Feasibility of the Zero-V: A Zero-Emission, Hydrogen Fuel-Cell, Coastal Research Vessel*; Sandia National Laboratories: Albuquerque, NM, USA, 2018; p. 325.
6. El Gohary, M.M.; Ammar, N.R.; Seddiek, I.S. Steam and SOFC based reforming options of PEM fuel cells for marine applications. *Brodogr. Teor. I Praksa Brodogr. I Pomor. Teh.* **2015**, *66*, 61–76.
7. Iulianelli, A.; Liguori, S.; Wilcox, J.; Basile, A. Advances on methane steam reforming to produce hydrogen through membrane reactors technology: A review. *Catal. Rev.* **2016**, *58*, 1–35. [[CrossRef](#)]
8. Yuan, J.; Ren, F.; Sundén, B. Analysis of chemical-reaction-coupled mass and heat transport phenomena in a methane reformer duct for PEMFCs. *Int. J. Heat Mass Transf.* **2007**, *50*, 687–701. [[CrossRef](#)]
9. Salemme, L.; Menna, L.; Simeone, M. Analysis of the energy efficiency of innovative ATR-based PEM fuel cell system with hydrogen membrane separation. *Int. J. Hydrog. Energy* **2009**, *34*, 6384–6392. [[CrossRef](#)]
10. Iulianelli, A.; Manzolini, G.; De Falco, M.; Campanari, S.; Longo, T.; Liguori, S.; Basile, A. H<sub>2</sub> production by low pressure methane steam reforming in a Pd-Ag membrane reactor over a Ni-based catalyst: Experimental and modeling. *Int. J. Hydrog. Energy* **2010**, *35*, 11514–11524. [[CrossRef](#)]
11. Authayanun, S.; Arpornwichanop, A.; Patcharavorachot, Y.; Wiyaratn, W.; Assabumrungrat, S. Hydrogen production from glycerol steam reforming for low-and high-temperature PEMFCs. *Int. J. Hydrogen Energy* **2011**, *36*, 267–275. [[CrossRef](#)]
12. Ahn, S.H.; Choi, I.; Kwon, O.J.; Kim, J.J. Hydrogen production through the fuel processing of liquefied natural gas with silicon-based micro-reactors. *Chem. Eng. J.* **2014**, *247*, 9–15. [[CrossRef](#)]
13. Hamid, M.K.A.; Ibrahim, N.; Ibrahim, K.A.; Ahmad, A. Simulation of hydrogen production for mobile fuel cell applications via autothermal reforming of methane. In Proceedings of the 1st International Conference on Natural Resources Engineering & Technology, Putrajaya, Malaysia, 24–25 July 2006; Citeseer: University Park, PA, USA, 2006.
14. Lin, S.-T.; Chen, Y.-H.; Yu, C.-C.; Liu, Y.-C.; Lee, C.-H. Modelling an experimental methane fuel processor. *J. Power Sources* **2005**, *148*, 43–53. [[CrossRef](#)]

15. Xu, J.; Froment, G.F. Methane steam reforming, methanation and water-gas shift: I. *Intrinsic kinetics*. *AIChE J.* **1989**, *35*, 88–96.
16. Nakagawa, N.; Sagara, H.; Kato, K. Catalytic activity of Ni-YSZ-CeO<sub>2</sub> anode for the steam reforming of methane in a direct internal-reforming solid oxide fuel cell. *J. Power Sources* **2001**, *92*, 88–94. [[CrossRef](#)]
17. Clarke, S.H.; Dicks, A.; Pointon, K.; Smith, T.A.; Swann, A. Catalytic aspects of the steam reforming of hydrocarbons in internal reforming fuel cells. *Catal. Today* **1997**, *38*, 411–423. [[CrossRef](#)]
18. Dicks, A.L. Hydrogen generation from natural gas for the fuel cell systems of tomorrow. *J. Power Sources* **1996**, *61*, 113–124. [[CrossRef](#)]
19. Belyaev, V.; Politova, T.; Mar'ina, O.; Sobyenin, V. Internal steam reforming of methane over Ni-based electrode in solid oxide fuel cells. *Appl. Catal. A Gen.* **1995**, *133*, 47–57. [[CrossRef](#)]
20. Ahmed, K.; Foger, K. Kinetics of internal steam reforming of methane on Ni/YSZ-based anodes for solid oxide fuel cells. *Catal. Today* **2000**, *63*, 479–487. [[CrossRef](#)]
21. Achenbach, E.; Riensche, E. Methane/steam reforming kinetics for solid oxide fuel cells. *J. Power Sources* **1994**, *52*, 283–288. [[CrossRef](#)]
22. Heinzel, A.; Vogel, B.; Hübner, P. Reforming of natural gas—hydrogen generation for small scale stationary fuel cell systems. *J. Power Sources* **2002**, *105*, 202–207. [[CrossRef](#)]
23. Cheekatarla, P.K.; Finnerty, C. Reforming catalysts for hydrogen generation in fuel cell applications. *J. Power Sources* **2006**, *160*, 490–499. [[CrossRef](#)]
24. Meusinger, J.; Riensche, E.; Stimming, U. Stimming. Reforming of natural gas in solid oxide fuel cell systems. *J. Power Sources* **1998**, *71*, 315–320. [[CrossRef](#)]
25. Calise, F.; D'Accadia, M.D.; Palombo, A.; Vanoli, L. Simulation and exergy analysis of a hybrid solid oxide fuel cell (SOFC)–gas turbine system. *Energy* **2006**, *31*, 3278–3299. [[CrossRef](#)]
26. Peters, R.; Dahl, R.; Klüttgen, U.; Palm, C.; Stolten, D. Internal reforming of methane in solid oxide fuel cell systems. *J. Power Sources* **2002**, *106*, 238–244. [[CrossRef](#)]
27. Chaniotis, A.; Poulidakos, D. Modeling and optimization of catalytic partial oxidation methane reforming for fuel cells. *J. Power Sources* **2005**, *142*, 184–193. [[CrossRef](#)]
28. Akbari, M.; Ardakani, A.S.; Tadbir, M.A. A microreactor modeling, analysis and optimization for methane autothermal reforming in fuel cell applications. *Chem. Eng. J.* **2011**, *166*, 1116–1125. [[CrossRef](#)]
29. Hoang, D.; Chan, S. Modeling of a catalytic autothermal methane reformer for fuel cell applications. *Appl. Catal. A Gen.* **2004**, *268*, 207–216. [[CrossRef](#)]
30. Xu, J.; Froment, G.F. Methane steam reforming: II. Diffusional limitations and reactor simulation. *AIChE J.* **1989**, *35*, 97–103. [[CrossRef](#)]
31. Kim, S.H.; Nam, S.-W.; Lim, T.-H.; Lee, H.-I. Effect of pretreatment on the activity of Ni catalyst for CO removal reaction by water–gas shift and methanation. *Appl. Catal. B Environ.* **2008**, *81*, 97–104. [[CrossRef](#)]
32. Elnashaie, S.; Abashar, M. Steam reforming and methanation effectiveness factors using the dusty gas model under industrial conditions. *Chem. Eng. Process. Process Intensif.* **1993**, *32*, 177–189. [[CrossRef](#)]
33. Finnerty, C.M.; Coe, N.J.; Cunningham, R.H.; Ormerod, R. Carbon formation on and deactivation of nickel-based/zirconia anodes in solid oxide fuel cells running on methane. *Catal. Today* **1998**, *46*, 137–145. [[CrossRef](#)]
34. EUTech Scientific Engineering GmbH. *Thermodynamic System Library, Release 5.4*; EUTech Scientific Engineering GmbH: Aachen, Germany, 2016; p. 333.
35. O'Hayre, R.; Cha, S.-W.; Colella, W.; Prinz, F.B. *Fuel Cell Fundamentals*; Wiley & Sons: New York, NY, USA, 2016.
36. Larminie, J.; Dicks, A.; McDonald, M.S. *Fuel Cell Systems Explained*; Wiley: Chichester, UK, 2003; Volume 2.
37. Molochas, C.; Tsiakaras, P. Carbon Monoxide Tolerant Pt-Based Electrocatalysts for H<sub>2</sub>-PEMFC Applications: Current Progress and Challenges. *Catalysts* **2021**, *11*, 1127. [[CrossRef](#)]
38. Garbis, P.; Kern, C.; Jess, A. Kinetics and reactor design aspects of selective methanation of CO over a Ru/ $\gamma$ -Al<sub>2</sub>O<sub>3</sub> catalyst in CO<sub>2</sub>/H<sub>2</sub> rich gases. *Energies* **2019**, *12*, 469. [[CrossRef](#)]